VII. STATISTICAL COMMUNICATION THEORY

Prof. Y. W. Lee
A. G. Bose
J. Y. Hayase
K. L. Jordan
C. S. Lorens
S. D. Pezaris
K. H. Powers
R. E. Wernikoff

A. A THEOREM CONCERNING NOISE FIGURES

The noise figure theorem discussed in the Quarterly Progress Report, April 15, 1955 (pp. 29-31), established the greatest lower bound for the noise figure of an n-amplifying device (n-UNIT) system as equal to the minimum noise figure of a system using one of the amplifying devices provided that certain conditions hold. Among these conditions was the one that each amplifying device have an equivalent circuit consisting of separate input and output parts.

It is desirable to prove the theorem without this condition in order to include in the scope of the theorem a broader class of amplifying devices. This has been achieved and the theorem now has the more general form given below.

The new theorem concerns the single frequency noise figure of linear systems belonging to the class τ which have the general form shown in Fig. VII-1. They consist of a given signal source S, n given amplifying devices (UNITS U_1 through U_n), and a coupling network. The class τ is determined by the signal source S and the UNITS 1 through n (that is, each system in τ has the same signal source and the same set of UNITS). It consists of the systems that are formed by all possible interconnections of the signal source and the n UNITS and satisfy conditions (a) through (e) below.

The one-to-one ideal transformers shown in Fig. VII-1 have the purpose of insuring that whatever signal is transmitted through a UNIT actually appears across its input terminals. Alternatively, any other scheme which achieves this result can be used, for example, grounding one input terminal of each UNIT.

Any system T belonging to τ satisfies the following conditions: (a) All noise generated within the system can be represented, for single frequency noise figure calculations, by ensembles of constant voltage and constant current generators located within the system. We shall refer to these generators as noise generators. (b) If these noise generators are grouped into n + 2 groups, according to whether they are located within the signal source S, the UNITS 1 through n, or in the coupling network C, no correlation exists between any two noise generators belonging to different groups. However, correlation may exist among noise generators of any one group. (c) The open-circuit transfer impedance of each UNIT from its input to its output terminals is not zero. (d) The coupling network C is such that when the system is excited by the signal source noise generator or any noise generator located within UNITS 1 through n the transmission from the input to the output circuits of the UNITS through C does not appreciably bypass the transmission through the UNITS themselves; any coupling through C between these input and output circuits is, effectively, a unilateral feedback from output to input.

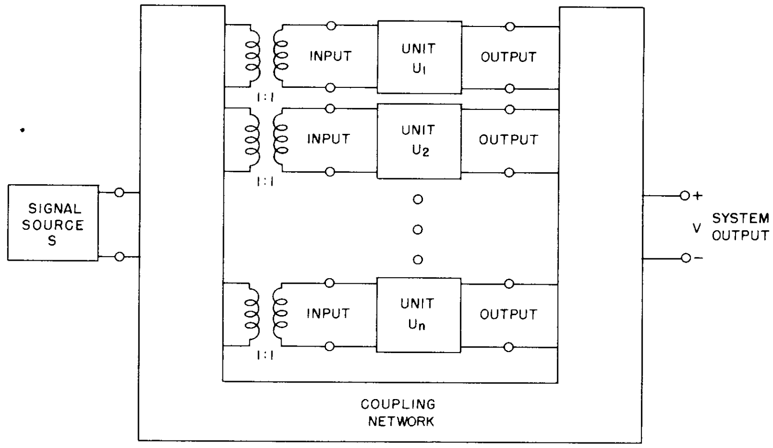

Fig. VII-1. The general form of a system belonging to the class τ

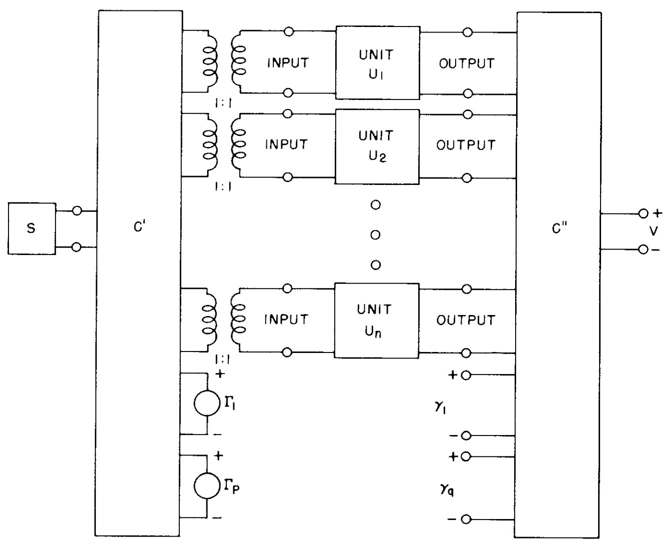

Fig. VII-2. System T'

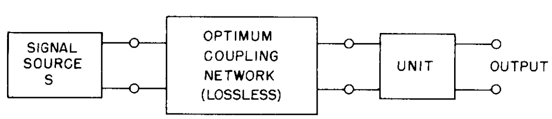

Fig. VII-3. A one-UNIT system with coupling network chosen to minimize the noise figure of the system

More precisely, C is such that a related system T', of the form shown in Fig. VII-2, exists whose transmission from the signal source or from any noise generator within the UNITS to the output is essentially the same as the corresponding transmission in the original system T. The original coupling from the output to the input circuits in T is represented in T' by the controlled voltage (or current sources Γ_1 through Γ_p, linearly related to the control voltages (or currents) γ_1 through γ_q. (e) The coupling network C' of T' is a passive, bilateral network.

The above conditions determine the class τ and the theorem is formulated as follows.

THEOREM: Given a signal source S and n UNITS the greatest lower bound of the noise figures of the systems belonging to the corresponding class τ (that is, the systems formed by arbitrary interconnections of S and the UNITS and satisfying conditions (a) through (e) is equal to the minimum noise figure attainable with a one-UNIT system of the form shown in Fig. VII-3 consisting of the same signal source, the "least noisy" one of the UNITS and a lossless coupling network with no feedback external to the UNIT. The "least noisy" UNIT referred to is that UNIT which when used in a system of the form of Fig. VII-3 yields a minimum noise figure which is at least as small as the minimum noise figure attainable with any of the remaining UNITS.

A. G. Bose, S. D. Pezaris

B. AN EXTENSION OF THE WIENER THEORY OF NONLINEAR SYSTEMS

We shall describe an extension of the Wiener theory of nonlinear system classification and representation that enables us to determine experimentally an optimum nonlinear filter. The theoretical as well as the experimental aspects of the problem are best described if, before proceeding to the general case, we first examine the special case of no-storage nonlinear filters.

1. The No-Storage Nonlinear Filter

Let x(t) and z(t) be the given filter input and the desired filter output time functions, respectively. We shall consider only bounded, continuous time functions. (This is clearly no restriction in the practical case.) Since x(t) is bounded, there exists an a and b such that $a \leqslant x(t) \leqslant b$ for all t. Now consider a set of n functions $\phi_j(x)$ $(j = 1, \ldots, n)$ over the interval (a,b). These functions have the property

$$\phi_j(x) = \begin{cases} 1 \text{ for } x_j - \frac{w}{2} \leqslant x < x_j + \frac{w}{2} \\ 0 \text{ for all other } x \end{cases} \qquad \left(w = \frac{b-a}{n}\right) \tag{1}$$

illustrated in Fig. VII-4. Clearly, this set of functions is orthogonal over the interval (a, b). We shall refer to these functions as "gate functions."

In the case of stationary no-storage filters the filter output y(t) at any instant is a unique function of the value of the input x(t) at the same instant. For reasons that will soon become apparent it is convenient to represent this output-input characteristic (transfer characteristic) of the no-storage filter in terms of an expansion employing the set of orthogonal functions defined above. We thus have

$$y(t) = \sum_{j=1}^{n} a_j \phi_j \left[x(t)\right] \tag{2}$$

The determination of an optimum no-storage filter for a given error criterion consists of choosing the a_j's in such a manner that the error between y(t) and the desired output z(t) is a minimum. We adopt a weighted mean square error criterion in which the weighting factor G(t) is a variable at our disposal. More specifically we minimize the integral

$$\mathcal{E} = \lim_{T\to\infty} \frac{1}{2T} \int_{-T}^{T} G(t) \left\{z(t) - \sum_{j=1}^{n} a_j \phi_j \left[x(t)\right]\right\}^2 dt \tag{3}$$

with respect to the n coefficients a_j.

Proceeding with the minimization and denoting the operation of time averaging by a bar above the averaged variable we have

$$\overline{G(t)\, \phi_k \left[x(t)\right] \left\{z(t) - \sum_{j=1}^{n} a_j \phi_j \left[x(t)\right]\right\}} = 0 \qquad (k = 1, \dots, n) \tag{4}$$

or

$$\overline{G(t)\, \phi_k \left[x(t)\right] \sum_{j=1}^{n} a_j \phi_j \left[x(t)\right]} = \overline{z(t)\, G(t)\, \phi_k \left[x(t)\right]} \tag{5}$$

It is readily seen that as a consequence of the non-overlapping property of the gate functions along the x-axis the $\phi_j \left[x(t)\right]$ $(j = 1, \dots, n)$ will, for single valued input time functions x(t), form an orthogonal set in time as well as in x and further that this orthogonality holds for any bounded weighting function. (For stationary time functions this is formally seen by using the ergodic theorem to evaluate $\overline{G(t)\, \phi_j \left[x(t)\right] \phi_k \left[x(t)\right]}$ on the ensemble basis.) Taking advantage of this time domain orthogonality, Eq. 5 reduces to

$$a_k \overline{G(t)\, \phi_k^2 \left[x(t)\right]} = \overline{z(t)\, G(t)\, \phi_k \left[x(t)\right]} \tag{6}$$

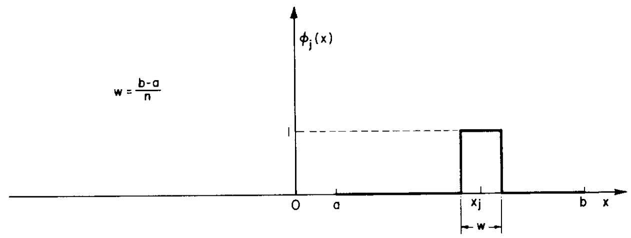

Fig. VII-4. Gate function $\phi_j(x)$

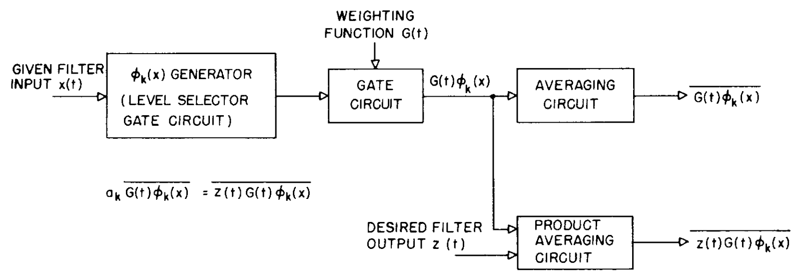

Fig. VII-5. Experimental setup for determination of optimum filter coefficients for the no-storage filter

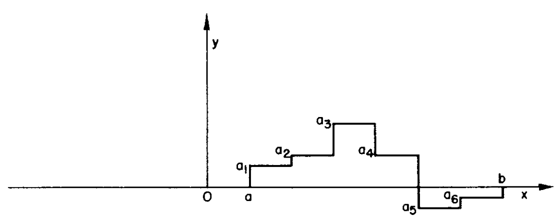

Fig. VII-6. Example of stepwise representation of a transfer characteristic over the interval (a, b). The a_k's are the optimum filter coefficients evaluated by the procedure indicated in Fig. VII-5

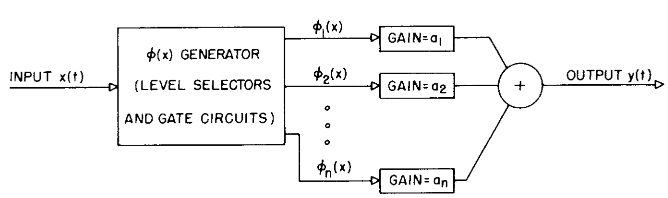

Fig. VII-7. Example of the formal synthesis of the no-storage filter according to Eq. 2

It follows from the definition of the $\phi_j(x)$ given in Eq. 1 that $\phi_j^2\left[x(t)\right] = \phi_j\left[x(t)\right]$ so that Eq. 6 can be rewritten as follows

$$a_k \overline{G(t)\,\phi_k\left[x(t)\right]} = \overline{z(t)\,G(t)\,\phi_k\left[x(t)\right]} \tag{7}$$

Equation 7 provides a convenient means of obtaining the desired coefficients a_k from measurements involving the given filter input, the desired filter output, and the error weighting time functions. The experimental setup for the evaluation of the coefficients is shown in Fig. VII-5.

From a knowledge of the coefficients a_k we can directly construct a stepwise approximation, like that of Fig. VII-6, to the desired optimum transfer characteristic. By increasing the number n of gate functions in a given region (a, b) of x we clearly get a better and better approximation to the transfer characteristic of the optimum no-storage filter.

The synthesis of the filter can be carried out formally according to Eq. 2 by using gate circuits and an adder as shown in Fig. VII-7, or we can synthesize the optimum characteristic by any of the other available techniques such as piecewise linear approximations or function generators.

In the discussion above it was assumed for convenience that each gate function had the same width w. We need not restrict ourselves to gate functions of equal width however. It is sufficient to choose them so that they cover the interval (a, b) and do not overlap. Thus if we have some a priori knowledge about the optimum transfer characteristic we may be able to save time and work in determining the characteristic by judiciously choosing the widths of the $\phi_j(x)$'s. In fact, after evaluating any number m of the a_k's we are free to alter the widths of the remaining functions $\phi_j(x)$ $(j > m)$ as we proceed. Thus, for example, in evaluating the a_k's if we find that they are not changing much from one to the next we can choose larger widths for the succeeding gate functions and in regions in which there is a large change between successive a_k's we can choose smaller widths to improve the accuracy. This flexibility is permissible because in taking advantage of it we do not disturb the time domain orthogonality of the gate functions.

2. The General Nonlinear Filter Involving Storage

Having investigated the special case of no-storage optimum filters we are now prepared to consider the general nonlinear filter involving storage. The difference is that no-storage systems operate only on the present value of the input while the general filter operates upon the past as well as on the present of the input. As discussed in the Quarterly Progress Report, October 15, 1954, page 57 we shall represent the past of the filter input $x(t)$ by the corresponding set of Laguerre coefficients $(u_1, \ldots, u_s)$. (The coefficients of other complete sets of orthogonal functions can be used in place of the Laguerre coefficients if desired.) The filter output y(t) is then some function of the Laguerre coefficients of the past of the input. We can write

$$y(t) = F\left[u_1, u_2, \ldots, u_s\right] \tag{8}$$

As in the case of the no-storage filter we are considering only bounded filter inputs. It can be shown, from the fact that the Laguerre functions are absolutely integrable, that the Laguerre coefficients of the past of x(t) are bounded if x(t) is bounded. Hence it is convenient to expand Eq. 8 in terms of gate functions whose arguments are the Laguerre coefficients. The expansion reads

$$y(t) = \sum_i \sum_j \cdots \sum_h a_{i,j,\ldots,h}\, \phi_i(u_1)\, \phi_j(u_2) \ldots \phi_h(u_s) \tag{9}$$

If $\Phi(x)$ represents the function $\phi_i(u_1)\, \phi_j(u_2) \ldots \phi_h(u_s)$ and A_α represents the corresponding value of $a_{i,j,\ldots,h}$ Eq. 9 takes the simplified form

$$y(t) = \sum_\alpha A_\alpha\, \Phi(\alpha) \tag{10}$$

As in the case of the no-storage filter (Eq. 3) we adopt a weighted mean square error criterion and minimize the integral

$$\mathscr{E} = \lim_{T\to\infty} \frac{1}{2T} \int_{-T}^{T} G(t) \left\{ z(t) - \sum_\alpha A_\alpha\, \Phi(\alpha) \right\}^2 dt \tag{11}$$

with respect to the coefficients A_α.

Now it is convenient to think in terms of an s-dimensional function space of the past of the input in which the axes are the unit Laguerre coefficients $\vec{u}_1$ through $\vec{u}_s$ of the past of the input. In this function space the past of the input is represented as a point corresponding to the tip of the vector formed by the Laguerre coefficients. As time progresses this point travels around in the function space.

Next let us consider $\Phi(\alpha)$ in the light of the function space discussed above. Since it is a product of gate functions of the different co-ordinates u_1 through u_s (compare Eq. 9 and Eq. 10), it has the value unity in one s-dimensional cell of the function space and zero elsewhere. The set of $\Phi(\alpha)$'s covers the function space in non-overlapping cells. As a consequence, the $\Phi(\alpha)$'s are orthogonal in time and furthermore this orthogonality holds with respect to any bounded weighting function.

Taking advantage of this time-domain orthogonality we can, by a procedure similar to that used in the no-storage case, minimize Eq. 11 with the result that the optimum

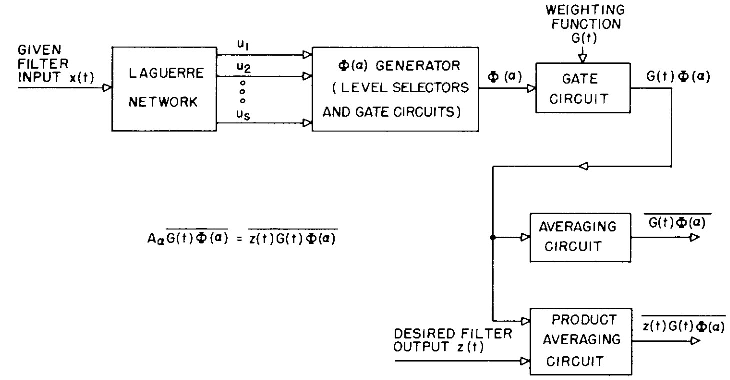

Fig. VII-8. Experimental setup for the determination of the general optimum filter involving storage

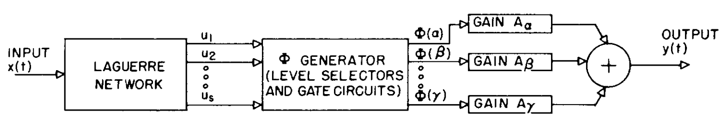

Fig. VII-9. Synthesis of the general optimum filter according to Eq. 10

coefficients A_a are given by relations of the form

$$A_a \overline{G(t)\ \Phi(a)} = \overline{z(t)\ G(t)\ \Phi(a)} \tag{12}$$

This relation provides a convenient means for experimentally determining the optimum coefficients. The apparatus for their determination is indicated in Fig. VII-8. Having determined the optimum coefficients, the nonlinear system can be synthesized according to Eq. 10 as indicated in Fig. VII-9.

In the procedure described above for determining and synthesizing optimum filters the use of gate functions in the expansion of Eq. 8 is of central importance. Let us examine some of the consequences of this:

1. The use of gate functions provides us with a series representation for the output of the filter in which the time domain orthogonality of the terms of the series is independent of the filter input. This enables us to obtain the optimum filter coefficients for arbitrary filter inputs without solving simultaneous equations.

2. Since the gate functions are orthogonal with respect to any weighting factor we can determine optimum filters for weighted mean square error criteria.

3. In most series representations of a function we encounter the difficulty that over some region of the independent variable small differences of two or more large terms are necessary to represent the desired function. In the gate function expansion Eq. 10

only one term has a non-zero value at any one instant of time; so this difficulty does not arise.

4. In general, the expansion of Eq. 8 involves the use of multipliers in the experimental setup. (For example, if a Taylor series or Hermite function expansion is used.) The use of gate functions replaces the multipliers by simpler level selectors and gate circuits.

NOTE: Because of the difficulties encountered in transforming a general filter input into a multivariate gaussian input, work on the method described in the Quarterly Progress Report, July 15, 1955, p. 38, has been temporarily discontinued in favor of the present method.

A. G. Bose

C. PROPERTIES OF SECOND-ORDER AUTOCORRELATION FUNCTIONS

1. Periodic Functions

If $f_1(t)$ of period T_1 has a Fourier expansion, and $F(n)$ is the complex line spectrum, then the second-order autocorrelation function of $f_1(t)$ is

$$\phi_{111}^*(\tau_1, \tau_2) = \frac{1}{T_1} \int_0^{T_1} f_1(t)\, f_1(t+\tau_1)\, f_1(t+\tau_2)\, dt$$

$$= \sum_{n_1=-\infty}^{\infty} \sum_{n_2=-\infty}^{\infty} F(n_1)\, F(n_2)\, \overline{F(n_1+n_2)}\, e^{j\omega_1(n_1\tau_1+n_2\tau_2)} \qquad (1)$$

By extracting the terms that correspond to $n_1 = 0$, $n_2 = 0$, and $n_1 = -n_2$, and using the relation

$$\phi_{11}(\tau) = \sum_{n=-\infty}^{\infty} |F(n)|^2\, e^{j\omega_1 n\tau} \qquad (2)$$

Eq. 1 can be rewritten as

$$\phi_{111}^*(\tau_1, \tau_2) = F(0)\left\{\phi_{11}(\tau_1) + \phi_{11}(\tau_2) + \phi_{11}(\tau_1 - \tau_2)\right\} - 2F^3(0)$$

$$+ \sum_{\substack{n_1=-\infty \\ \left(\substack{n_1\neq 0,\ n_2\neq 0 \\ n_1\neq -n_2}\right)}}^{\infty} \sum_{n_2=-\infty}^{\infty} F(n_1)\, F(n_2)\, \overline{F(n_1+n_2)}\, e^{j\omega_1(n_1\tau_1+n_2\tau_2)} \qquad (3)$$

This expression shows that the second-order autocorrelation function of a periodic function is the sum of first-order autocorrelation functions that are free of phase relationship of the harmonics, a double summation term that involves the phase relationship of the harmonics, and a constant term.

The last term in Eq. 3 can be rewritten by adding the terms with positive n_1, n_2 to the corresponding terms with negative n_1, n_2. These terms are complex conjugates. Also the terms that correspond to $n_1 > 0$, $n_2 < 0$, and $n_1 < 0$, $n_2 > 0$ are complex conjugates, and they will be added. When this is done Eq. 3 becomes

$$\phi_{111}^{*}(\tau_1,\tau_2) = F(0)\left\{\phi_{11}(\tau_1) + \phi_{11}(\tau_2) + \phi_{11}(\tau_1 - \tau_2)\right\} - 2F^3(0)$$
$$+ 2\sum_{n_1=1}^{\infty}\sum_{n_2=1}^{\infty} \mathrm{Re}\left[F(n_1)\,F(n_2)\,\overline{F(n_1+n_2)}\,e^{j\omega_1(n_1\tau_1+n_2\tau_2)}\right]$$
$$+ 2\sum_{n_1=1}^{\infty}\sum_{\substack{n_2=1\\(n_1\neq n_2)}}^{\infty} \mathrm{Re}\left[F(n_1)\,F(-n_2)\,\overline{F(n_1-n_2)}\,e^{j\omega_1(n_1\tau_1-n_2\tau_2)}\right] \qquad (4)$$

The complex line spectrum F(n) can be expressed as

$$F(n) = \frac{a_n - jb_n}{2} \qquad (5)$$

where a_n and b_n are twice the average of $f_1(t)\cos n\omega_1 t$ and $f_1(t)\sin n\omega_1 t$ over the interval $(0, T_1)$ respectively.

If $f_1(t)$ is an odd periodic function, $F(0) = 0$, $F(n) = -jb_n/2$ when $n \neq 0$. In this case Eq. 4 becomes

$$\phi_{111}^{*}(\tau_1,\tau_2) = \frac{1}{4}\left[\sum_{n_1=1}^{\infty}\sum_{n_2=1}^{\infty} b_{n_1}\, b_{n_2}\, b_{n_1+n_2}\sin\omega_1(n_1\tau_1 + n_2\tau_2)\right.$$
$$\left. + \sum_{n_1=1}^{\infty}\sum_{\substack{n_2=1\\(n_1\neq n_2)}}^{\infty} b_{n_1}\, b_{-n_2}\, b_{n_1-n_2}\sin\omega_1(n_1\tau_1 - n_2\tau_2)\right] \qquad (6)$$

Equation 6 shows that the second-order autocorrelation function of an odd periodic function does not involve first-order terms, and vanishes at $\tau_1 = \tau_2 = 0$.

When $f_1(t)$ is an even periodic function, $F(n) = a_n/2$, and Eq. 4 becomes

$$\phi^*_{111}(\tau_1,\tau_2) = \frac{a_o}{4}\left[\sum_{n_1=1}^{\infty} a_{n_1}^2 \cos\omega_1 n_1\tau_1 + \sum_{n_2=1}^{\infty} a_{n_2}^2 \cos\omega_1 n_2\tau_2 + \sum_{n=1}^{\infty} a_n^2 \cos\omega_1 n(\tau_1 - \tau_2)\right] + \left(\frac{a_o}{2}\right)^3$$
$$+ \frac{1}{4}\left[\sum_{n_1=1}^{\infty}\sum_{n_2=1}^{\infty} a_{n_1} a_{n_2} a_{n_1+n_2} \cos\omega_1(n_1\tau_1 + n_2\tau_2) + \sum_{\substack{n_1=1 \\ (n_1\neq n_2)}}^{\infty}\sum_{n_2=1}^{\infty} a_{n_1} a_{-n_2} a_{n_1-n_2} \cos\omega_1(n_1\tau_1 - n_2\tau_2)\right] \tag{7}$$

The second-order autocorrelation function of an even periodic function is symmetrical about the lines $\tau_1 = -\tau_2$ and $\tau_1 = \tau_2$. The proof is established by the relationships

$$\phi^*_{111}(\tau_1,\tau_2) = \phi^*_{111}(\tau_2,\tau_1) \tag{8}$$

$$\phi^*_{111}(\tau_1,\tau_2) = \phi^*_{111}(-\tau_1,-\tau_2) \tag{9}$$

which hold in Eq. 7. From Eq. 8 the values of $\phi^*_{111}(\tau_1,\tau_2)$ at points A and B of Fig. VII-10 are equal. Similarly, the values of $\phi^*_{111}(\tau_1,\tau_2)$ at points C and D are equal. From Eq. 9 the values of $\phi^*_{111}(\tau_1,\tau_2)$ at points A and D are equal. Hence in the first and third quadrants $\phi^*_{111}(\tau_1,\tau_2)$ is symmetrical about the line $\tau_1 = -\tau_2$.

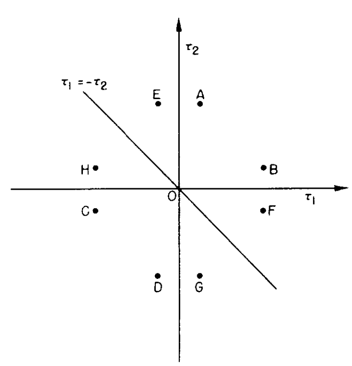

Fig. VII-10. τ_1, τ_2-plane

From Eq. 8, the values of $\phi^*_{111}(\tau_1, \tau_2)$ at points E and F are equal. From relation 9, the values of $\phi^*_{111}(\tau_1, \tau_2)$ at points E and G are equal. Hence the values of $\phi^*_{111}(\tau_1, \tau_2)$ at points F and G are equal. This shows that $\phi^*_{111}(\tau_1, \tau_2)$ is symmetrical about $\tau_1 = -\tau_2$ in the fourth quadrant. The use of relation 9 shows that the values of $\phi^*_{111}(\tau_1, \tau_2)$ at points F and H are equal. Hence the values of $\phi^*_{111}(\tau_1, \tau_2)$ at points E and H are equal. This shows that the line $\tau_1 = -\tau_2$ is the line of symmetry in the second quadrant.

Relation 8 is used to prove that $\phi^*_{111}(\tau_1, \tau_2)$ is symmetrical about $\tau_1 = \tau_2$ in all the quadrants.

2. Aperiodic Functions

If $f_1(t)$ is an aperiodic function, and $F(\omega)$ is its Fourier transform, the second-order autocorrelation function of $f_1(t)$ is

$$\phi^*_{111}(\tau_1, \tau_2) = \int_{-\infty}^{\infty} f_1(t)\, f_1(t+\tau_1)\, f_1(t+\tau_2)\, dt$$

$$= 2\pi \int_{-\infty}^{\infty}\int_{-\infty}^{\infty} F(\omega_1)\, F(\omega_2)\, \overline{F(\omega_1+\omega_2)}\, e^{j(\omega_1\tau_1+\omega_2\tau_2)}\, d\omega_1\, d\omega_2$$

$$= \int_{-\infty}^{\infty}\int_{-\infty}^{\infty} \Phi^*(\omega_1, \omega_2)\, e^{j(\omega_1\tau_1+\omega_2\tau_2)}\, d\omega_1\, d\omega_2 \qquad (10)$$

where

$$\Phi^*(\omega_1, \omega_2) = 2\pi\, F(\omega_1)\, F(\omega_2)\, \overline{F(\omega_1+\omega_2)}$$

It is of interest to consider $\Phi^*(\omega_1, \omega_2)$ when $\omega_1 = 0$, when $\omega_2 = 0$, and when $\omega_1 = -\omega_2$. When $\omega_1 = 0$,

$$\Phi^*(0, \omega_2) = 2\pi\, F(0)\, |F(\omega_2)|^2 = F(0)\, \Phi_{11}(\omega_2) \qquad (11)$$

where $\Phi_{11}(\omega_2)$ is the energy density spectrum of $f_1(t)$. Similarly, when $\omega_2 = 0$,

$$\Phi^*(\omega_1, 0) = 2\pi\, F(0)\, |F(\omega_1)|^2 = F(0)\, \Phi_{11}(\omega_1) \qquad (12)$$

When $\omega_1 = -\omega_2$,

$$\Phi^*(\omega_1 = -\omega_2, \omega_2) = 2\pi\, F(-\omega_2)\, F(\omega_2)\, \overline{F(0)} = F(0)\, \Phi_{11}(\omega_2) \qquad (13)$$

To illustrate this point, the Fourier transforms of second-order autocorrelation functions of two aperiodic functions will be evaluated. The first function is,

$$f_1(t) = \begin{cases} E\, e^{-at} & \text{for } t \geqslant 0 \\ 0 & \text{for } t < 0 \end{cases} \tag{14}$$

where $a > 0$. The second-order autocorrelation function of this function is

$$\phi^*_{111}(\tau_1, \tau_2) = \begin{cases} \frac{E^3}{3a} e^{-a(\tau_1+\tau_2)} & \text{when } \tau_1 \geqslant 0,\ \tau_2 \geqslant 0 \\ \frac{E^3}{3a} e^{-a(\tau_1-2\tau_2)} & \text{when } \tau_1 > 0,\ \tau_2 < 0, \text{ and when } \tau_1 < 0,\ \tau_2 < 0, \text{ and } |\tau_2| > |\tau_1| \\ \frac{E^3}{3a} e^{a(2\tau_1-\tau_2)} & \text{when } \tau_1 < 0,\ \tau_2 > 0, \text{ and when } \tau_1 < 0,\ \tau_2 < 0, \text{ and } |\tau_1| > |\tau_2| \end{cases} \tag{15}$$

The transform $\Phi^*(\omega_1, \omega_2)$ of $\phi^*_{111}(\tau_1, \tau_2)$ is given by

$$\Phi^*(\omega_1, \omega_2) = \frac{1}{(2\pi)^2} \int_{-\infty}^{\infty} \int_{-\infty}^{\infty} \phi^*_{111}(\tau_1, \tau_2)\, e^{-j(\omega_1\tau_1+\omega_2\tau_2)}\, d\tau_1\, d\tau_2 \tag{16}$$

The evaluation of Eq. 16 can be simplified by utilizing the symmetry property of $\phi^*_{111}(\tau_1, \tau_2)$. From the definition of $\phi^*_{111}(\tau_1, \tau_2)$, it is readily seen that

$$\phi^*_{111}(\tau_1, \tau_2) = \phi^*_{111}(\tau_2, \tau_1) \tag{17}$$

and $\phi^*_{111}(\tau_1, \tau_2)$ is symmetrical about the line $\tau_1 = \tau_2$. First consider the evaluation of $\Phi^*(\omega_1, \omega_2)$ in the plane where $\tau_1 > 0$, $\tau_2 < 0$, and $\tau_1 < 0$, $\tau_2 > 0$. In the first region $\Phi^*(\omega_1, \omega_2)$ is

$$\frac{1}{(2\pi)^2} \int_{\tau_1=0}^{\infty} \int_{\tau_2=-\infty}^{0} \phi^*_{111}(\tau_1, \tau_2)\, e^{-j(\omega_1\tau_1+\omega_2\tau_2)}\, d\tau_2\, d\tau_1 \tag{18}$$

Letting $\tau_1 = \tau_2$, $\tau_2 = \tau_1$ and using Eq. 17, Eq. 18 becomes

$$\frac{1}{(2\pi)^2} \int_{\tau_2=0}^{\infty} \int_{\tau_1=-\infty}^{0} \phi^*_{111}(\tau_1, \tau_2)\, e^{-j(\omega_1\tau_2+\omega_2\tau_1)}\, d\tau_1\, d\tau_2 \tag{19}$$

In the τ_1, τ_2-plane, where $\tau_1 < 0$, $\tau_2 > 0$, $\Phi^*(\omega_1, \omega_2)$ is

$$\frac{1}{(2\pi)^2} \int_{\tau_1=-\infty}^{0} \int_{\tau_2=0}^{\infty} \phi^*_{111}(\tau_1, \tau_2)\, e^{-j(\omega_1\tau_1+\omega_2\tau_2)}\, d\tau_2\, d\tau_1 \tag{20}$$

Equations 19 and 20 are identical except for the interchange of ω_1 and ω_2, provided the order of integration with respect to τ_1 and τ_2 is interchangeable. From this we see that once $\Phi^*(\omega_1, \omega_2)$ has been evaluated in the region where $\tau_1 > 0$, $\tau_2 < 0$ we can obtain $\Phi^*(\omega_1, \omega_2)$ in the region where $\tau_1 < 0$, $\tau_2 > 0$ by interchanging ω_1 and ω_2 in the expression for $\Phi^*(\omega_1, \omega_2)$ in the first region.

In the τ_1, τ_2-plane where $\tau_1 > 0$, $\tau_2 > 0$, and $\tau_1 > \tau_2$, $\Phi^*(\omega_1, \omega_2)$ is

$$\frac{1}{(2\pi)^2} \int_{\tau_1=0}^{\infty} \int_{\tau_2=0}^{\tau_1} \phi_{111}^*(\tau_1, \tau_2)\, e^{-j(\omega_1\tau_1 + \omega_2\tau_2)}\, d\tau_2\, d\tau_1 \tag{21}$$

If we let $\tau_1 = \tau_2$, $\tau_2 = \tau_1$, and use Eq. 17, Eq. 21 becomes

$$\frac{1}{(2\pi)^2} \int_{\tau_2=0}^{\infty} \int_{\tau_1=0}^{\tau_2} \phi_{111}^*(\tau_1, \tau_2)\, e^{-j(\omega_1\tau_2 + \omega_2\tau_1)}\, d\tau_1\, d\tau_2 \tag{22}$$

In the τ_1, τ_2-plane where $\tau_1 > 0$, $\tau_2 > 0$, and $\tau_1 < \tau_2$, $\Phi^*(\omega_1, \omega_2)$ is

$$\frac{1}{(2\pi)^2} \int_{\tau_2=0}^{\infty} \int_{\tau_1=0}^{\tau_2} \phi_{111}^*(\tau_1, \tau_2)\, e^{-j(\omega_1\tau_1 + \omega_2\tau_2)}\, d\tau_1\, d\tau_2 \tag{23}$$

By comparing Eq. 22 and Eq. 23, we see that the two expressions are the same except that ω_1 and ω_2 have been interchanged. Hence, having obtained $\Phi^*(\omega_1, \omega_2)$ in the τ_1, τ_2-plane where $\tau_1 > 0$, $\tau_2 > 0$, and $\tau_1 > \tau_2$, we merely interchange ω_1 and ω_2 in this expression to obtain $\Phi^*(\omega_1, \omega_2)$ in the region where $\tau_1 > 0$, $\tau_2 > 0$, and $\tau_1 < \tau_2$.

The same reasoning is used to show that if $\Phi^*(\omega_1, \omega_2)$ has been obtained in the τ_1, τ_2-plane where $\tau_1 < 0$, $\tau_2 < 0$, and $|\tau_1| < |\tau_2|$, then by interchanging ω_1 and ω_2 in this expression we obtain $\Phi^*(\omega_1, \omega_2)$ in the τ_1, τ_2-plane where $\tau_1 < 0$, $\tau_2 < 0$, and $|\tau_1| > |\tau_2|$.

To evaluate $\Phi^*(\omega_1, \omega_2)$ of the function defined in Eq. 14 the preceding method will not be used, for it can be evaluated readily by substituting $\phi_{111}^*(\tau_1, \tau_2)$, as defined in Eq. 15, in Eq. 16 and performing the integration. When we do this

$$\Phi^*(\omega_1, \omega_2) = \frac{E^3}{4\pi^2} \frac{1}{a\left(a^2 + \omega_1\omega_2 + \omega_1^2 + \omega_2^2\right) + j\,\omega_1\omega_2(\omega_1 + \omega_2)} \tag{24}$$

Let $\omega_2 = 0$, then Eq. 24 becomes

$$\Phi^*(\omega_1, 0) = \frac{E}{2\pi a}\left(\frac{E^2}{2\pi a} \frac{a}{a^2 + \omega_1^2}\right) = F(0)\, \Phi_{11}(\omega_1) \tag{25}$$

where

$$F(0) = \frac{E}{2\pi a} \tag{26}$$

and the energy density spectrum of $f_1(t)$ defined in Eq. 14 is

$$\Phi_{11}(\omega_1) = \frac{E^2}{2\pi a} \frac{a}{a^2 + \omega_1^2} \tag{27}$$

Similarly when $\omega_1 = 0$ and $\omega_1 = -\omega_2$

$$\Phi^*(0, \omega_2) = \Phi^*(\omega_1 = -\omega_2, \omega_2) = \frac{E}{2\pi a} \left(\frac{E^2}{2\pi a} \frac{a}{a^2 + \omega_2^2} \right) = F(0)\, \Phi_{11}(\omega_2) \tag{28}$$

As a second example consider the function

$$f_1(t) = \begin{cases} E & \text{when } 0 \leqslant t \leqslant b \\ 0 & \text{elsewhere} \end{cases} \tag{29}$$

In evaluating $\Phi^*(\omega_1, \omega_2)$ for this case, we will use the property that $\phi^*_{111}(\tau_1, \tau_2)$ is symmetrical about $\tau_1 = \tau_2$. First we will find the expression for $\phi^*_{111}(\tau_1, \tau_2)$ below the line $\tau_1 = \tau_2$ in Fig. VII-11

$$\phi^*_{111}(\tau_1, \tau_2) = \begin{cases} E^3(b - \tau_1) & \text{when } \tau_1 > 0,\ \tau_2 > 0, \text{ and } \tau_1 > \tau_2 \\ E^3(b - \tau_1 - |\tau_2|) & \text{when } \tau_1 > 0,\ \tau_2 < 0 \\ E^3(b - |\tau_2|) & \text{when } \tau_1 < 0,\ \tau_2 < 0, \text{ and } |\tau_1| \leqslant |\tau_2| \end{cases} \tag{30}$$

Next we will evaluate Eq. 16 in regions I, II, and III in Fig. VII-11 and by interchanging ω_1 and ω_2 in these expressions we obtain the expressions for $\Phi^*(\omega_1, \omega_2)$ in regions VI, V,

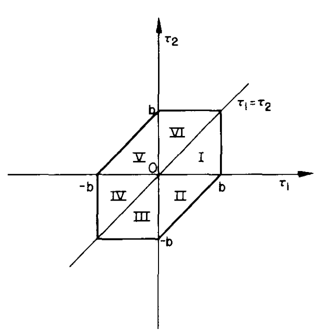

Fig. VII-11. Plane over which $\phi^*_{111}(\tau_1, \tau_2)$ in Eq. 30 is defined and IV. Summing the six expressions

$$\Phi^*(\omega_1, \omega_2) = \frac{E^3}{(2\pi)^2} \frac{-2 \sin(\omega_1 + \omega_2) b + 2 \sin\omega_1 b + 2 \sin\omega_2 b}{\omega_1\omega_2(\omega_1 + \omega_2)} \tag{31}$$

Application of L' Hôpital' s Rule gives

$$\lim_{\omega_1 \to 0} \Phi^*(\omega_1, \omega_2) = \left(\frac{Eb}{2\pi}\right) \left\{ \frac{E^2 b^2}{2\pi} \left(\frac{\sin \frac{\omega_2 b}{2}}{\frac{\omega_2 b}{2}} \right)^2 \right\} = F(0)\, \Phi_{11}(\omega_2) \tag{32}$$

where

$$F(0) = \frac{Eb}{2\pi} \tag{33}$$

and the energy density spectrum of $f_1(t)$ defined in Eq. 29 is

$$\Phi_{11}(\omega_2) = \frac{E^2 b^2}{2\pi} \left(\frac{\sin \frac{\omega_2 b}{2}}{\frac{\omega_2 b}{2}} \right)^2 \tag{34}$$

Since Eq. 31 is symmetrical with respect to ω_1 and ω_2,

$$\lim_{\omega_2 \to 0} \Phi^*(\omega_1, \omega_2) = F(0)\, \Phi_{11}(\omega_1) \tag{35}$$

L' Hôpital' s Rule is applied again to get

$$\lim_{\omega_1 \to -\omega_2} \Phi(\omega_1, \omega_2) = F(0)\, \Phi_{11}(\omega_2) \tag{36}$$

The preceding examples show that the second-order autocorrelation function of an aperiodic function includes the effects of the first-order autocorrelation when $F(0) \neq 0$. For the aperiodic function such that $F(0) = 0$, the effects of the first-order autocorrelation function are absent in the second-order autocorrelation function. An example of this is

$$f_1(t) = \begin{cases} E & \text{when } 0 \leqslant t \leqslant b \\ -E & \text{when } -b \leqslant t \leqslant 0 \\ 0 & \text{elsewhere} \end{cases} \tag{37}$$

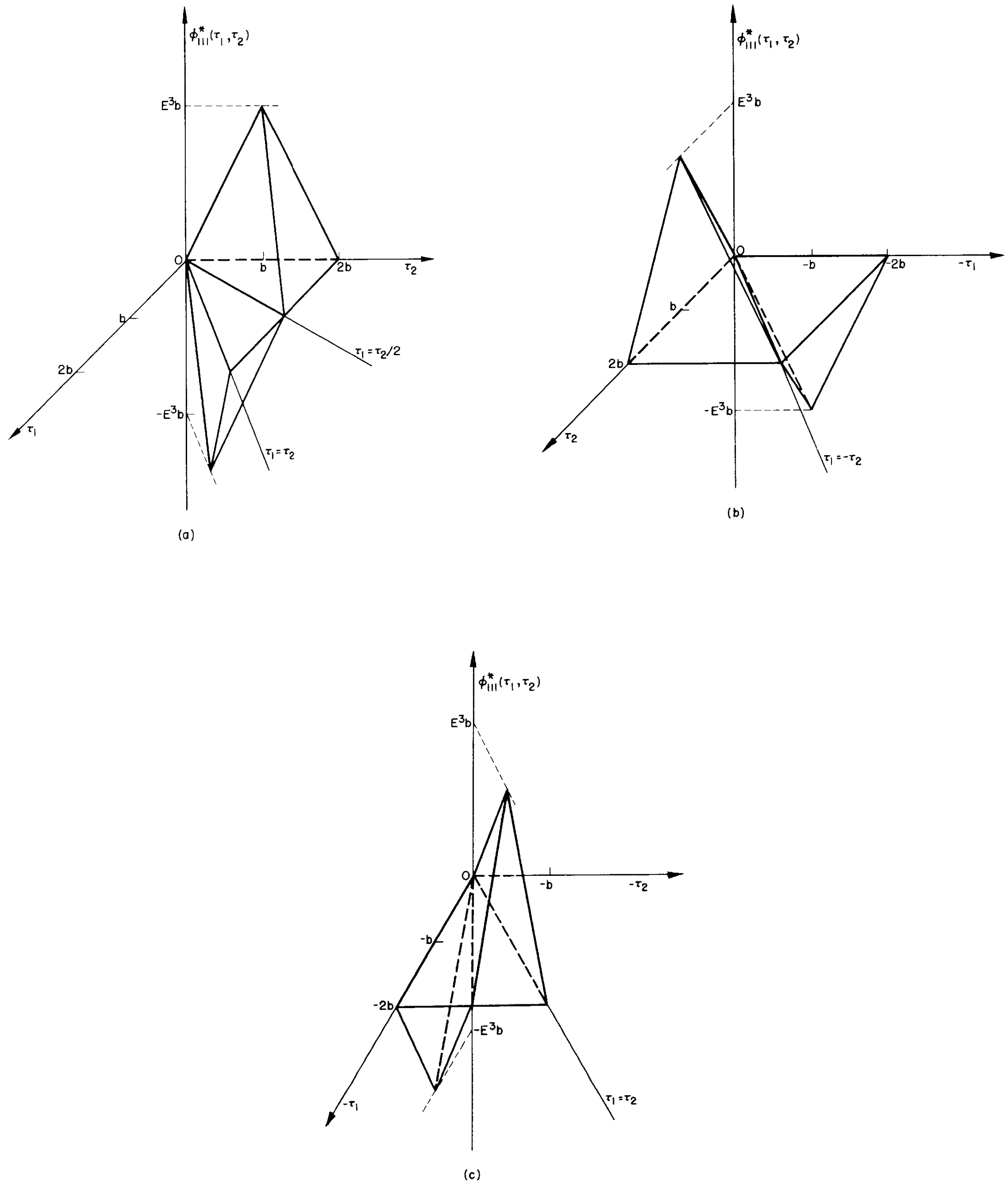

Fig. VII-12. a. Plot of $\phi^*_{111}(\tau_1,\tau_2)$ for $\tau_1 > 0$, $\tau_2 > 0$, $\tau_2 > \tau_1$ of $f_1(t)$ given by Eq. 37; b. Plot of $\phi^*_{111}(\tau_1,\tau_2)$ for $\tau_1 < 0$, $\tau_2 > 0$ of $f_1(t)$ given by Eq. 37; c. Plot of $\phi^*_{111}(\tau_1,\tau_2)$ for $\tau_1 < 0$, $\tau_2 < 0$, $|\tau_1| > |\tau_2|$ of $f_1(t)$ given by Eq. 37

The second-order autocorrelation function in this case vanishes at the origin and is nonzero within a certain region as shown in Fig. VII-12a, b, c.

J. Y. Hayase

D. AN ANALOG PROBABILITY DENSITY ANALYZER

A proposed analog probability density analyzer uses the principle described by W. Davenport in the Research Laboratory of Electronics Technical Report 148. Briefly this principle involves creating a time function g(t) whose value is unity whenever the amplitude of the time function x(t), of which the density is being measured, lies within a given interval E to E + ΔE and is zero otherwise. The time average of g(t) is then the probability that f(t) lies in the interval E to E + ΔE.

Figure VII-13 shows the essential elements of a system that provides a continuous plot of the amplitude probability density P(x) versus x. A modulation scheme is employed to avoid the use of direct-coupled amplifiers. By means of the variable resistor R_5 the voltage across A-B is adjusted, with no input to the probability analyzer, to a chosen value ΔE volts. A small synchronous motor is used to slowly drive the helipot R_3 so that the voltage E at point D increases linearly with time over a predetermined range. When the time function to be analyzed, x(t), is applied at the input to the tube T1, it is amplified and appears at point C. When the voltage at point C lies between E + ΔE/2 and E - ΔE/2 both diodes are open. When the voltage is outside of this range one of the two diodes is closed. If R_L is chosen to be much smaller than the resistance of the voltage divider (R_2, R_3, and R_4), the impedance to ground seen at points A and B when either diode is closed is very small compared to the value when both diodes are open.

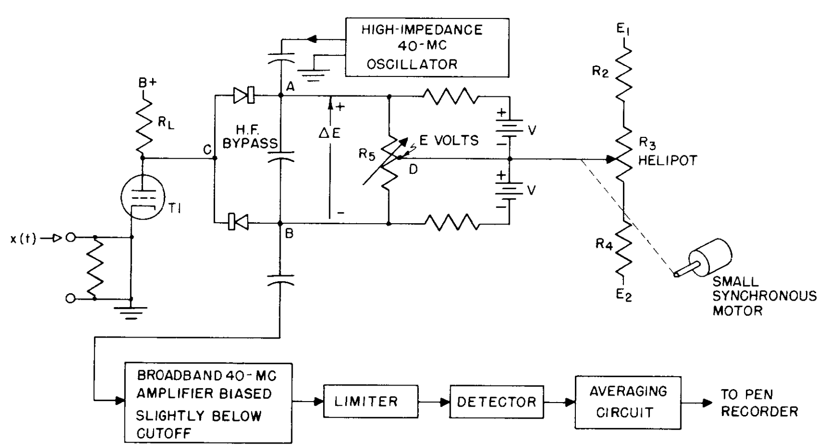

Fig. VII-13. Essential features of the proposed analog probability density analyzer

Connected to point A is a high-impedance, high-frequency (ca., 40-Mc) oscillator. The oscillator voltage at point A, with both diodes open, is negligibly small compared to the magnitude of the signal voltage variation at point C. This condition is necessary so that the oscillator voltage does not influence the closing of the diodes. The 40-Mc signal at point A or B will be much larger when both diodes are open than when either diode is closed. This 40-Mc signal at point B is fed into an amplifier which is biased slightly below cutoff so that it gives an output only when both diodes are open. The output of the amplifier is limited and detected, yielding a time function proportional to g(t) described above. The output of the detector is then averaged and fed directly to a pen recorder.

The method described above can be easily extended to the measurement of second probability densities.

A. G. Bose